THE UNIVERSITY OF TEXAS
AT ARLINGTON

Effects of Graphene in High-Density Polyethylene Microfibers

By

ASHISH LAL SIVADAS ANILAL

December 2022

Presented to the Faculty of the Graduate School of The University of Texas at Arlington in Partial Fulfillment of the requirements for the Degree of **MASTER OF SCIENCE IN MATERIALS SCIENCE AND ENGINEERING** (Thesis-Concentration)

Supervising Committee:

Dr. Michael Bozlar
Dr. Erika La Plante
Dr. Kyung Suk Yum
Dr. Robin Macaluso

Acknowledgements

December 5, 2022

I would like to thank the University of Texas at Arlington for accepting me as a Graduate Student and allowing me to pursue my Master's in Materials Science and Engineering.

I would like to thank Dr. Michael Bozlar for allowing me to do my thesis in his lab. I have upskilled and learnt a lot during my time with him. I will always value the guidance and tips he has given me in improving my work.

I would like to thank Dr. Erika La Plante, Dr. Kyung Suk Yum, and Dr. Robin Macaluso for agreeing to be on my Thesis Defense Committee and examining my work out of their busy schedules.

I would like to thank Dr. Seong Jin Koh for advising me throughout my Masters' journey.

I would like to thank my fellow lab mates Mr. Sean Menezes, Mr. Nitish Kallakuri, Mr. Piyush Parab, Mr. Noel Johnson, and Mr. Luqman Charolia for their assistance and help extended during my experiments.

Lastly, I would like to thank my parents Mr. Anilal, Mrs. Shalini Anilal and my brother Mr. Adarsh Anilal for trusting me and supporting me through this journey.

ABSTRACT

EFFECTS OF GRAPHENE IN HIGH-DENSITY POLEYTHYLENE MICROFIBERS

ASHISH LAL SIVADAS ANILAL

Materials Science and Engineering

The University of Texas at Arlington, 2022

Thesis Advisor: Dr Michael Bozlar

High-Density Polyethylene uniquely can induce banded spherulites as it is crystallized from its melt. We studied the effects of graphene in the crystallography of banded HDPE by examining parameters such as the extent of twisting, spherulitic growth, and nucleation density. The application of graphene as a multifunctional filler in polymer matrices is a great topic of interest because graphene at low concentrations can bring many improvements in mechanical, electrical, and thermal properties. We synthesized graphene oxide by chemical oxidation of graphite and further studied its effects in the twisted crystallography of HDPE. Three batches of fibers were extruded: two batches with different concentrations of graphene and a neat HDPE for cross-examination. The HDPE microfibers were produced using a twin-screw extruder/micro-compounder. The fibers were analyzed using characterization techniques such as Polarized Optical Microscopy, Scanning Electron Microscopy and X-Ray Diffraction.

List of Figures

Table of Content

Chapter 1: Introduction

1.1 Polyethylene

Polyethylene (PE) is a thermoplastic polymer with variable crystallography and a vast spectrum of applications. Today, PE is one of the most popular and used plastic for commercial applications with tens of millions of productions across the globe. It is cost-effective and can be found everywhere, from grocery stores to medical devices. PE accounts for 36% of the total polymer production followed by polypropylene.[1]

PE falls under the polyolefin family with the chemical formula $(C_2H4)n$. It is synthesized by polymerizing ethylene gas.[2] It has good processability, mechanical properties, commendable vapor barrier functions, gas barrier properties, and many more.[3] PE can be classified in terms of molecular weight, branching, and crystal structure.[4] It is further categorized into the following subdivisions.

i. Low-Density Polyethylene (LDPE)

LDPE is a hydrophilic polymer with exceptionally good strength and tensile properties.[5] It also has an excellent tear, good impact strength, and stress-cracking resistance.[6] LDPE has the most branching when compared to its counterparts.[7] LDPE has the highest degree of branching with short and long chains.[8] It was one of the primary polymers to emerge as a component for packaging in the early 1940s, with its highly branched crystallography, lower density, and good clarity.[9,10] Figure 1.1.1 shows the morphology of the polymer chains in LDPE.

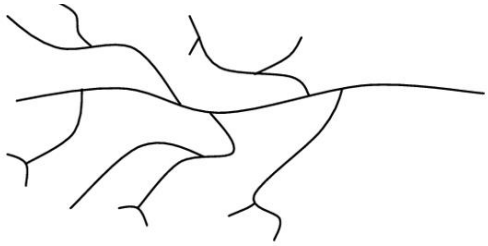

Figure 1. Morphological Diagram of LDPE[11]

ii. Linear Low-Density Polyethylene (LLDPE)

LLDPE has a denser structure compared to LDPE. It is a soft, flexible material with a haze in appearance.[12] LLDPE has high degree of branching with short chains.[8] It is also a hydrophilic polymer with high tensile, low bending stiffness, and other barrier properties.[5,13] Like LDPE, LLDPE is also used as films, in the packaging industry, heat seal coatings considering the range of properties it exhibits.[14] Figure 1.1.2 shows the morphological diagram of LLDPE.

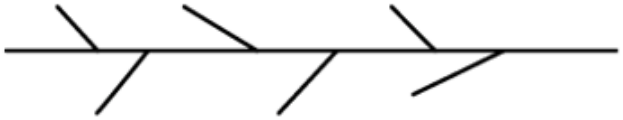

Figure 1.1.2 Morphological Diagram of LLDPE[11]

iii. High-Density Polyethene (HDPE)

HDPE is a linear addition polymer of ethylene synthesized at temperatures and pressures the same as LLDPE.[12] It is the least branched polyethylene type with the reputation of being the engineering polymer. HDPE is the most preferred plastic for applications such as food packaging, bottles, and other commercial containers. Unlike LDPE and LLDPE the degree of branching is comparatively very low with very short chains. Due to its impact resistance, strength, and chemical resistance, it is also a suitable candidate for industrial chemical containers.[15] Figure 1.1.4 shows a morphological diagram of HDPE.

Figure 1.1.3 Morphological Diagram of HDPE[11]

iv. Ultra High Molecular Weight Polyethylene (UHMW-PE)

UHMW-PE is strong and light with exceptionally low density and its fiber composites are widely used in high-performance ballistic applications.[16] It is extensively used for total joint replacements because it combines excellent wear resistance, strength, and biocompatibility.[17] The UHMW-PE fibers, a kind of polyolefin fiber, are usually

synthesized by gel spinning.[16] Figure 1.1.5 shows a morphological diagram of UHWM-PE.

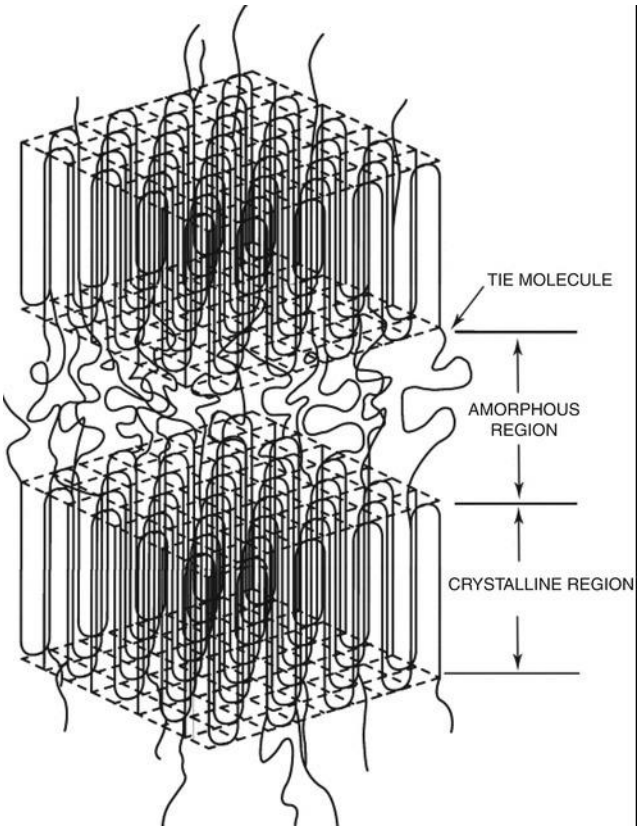

Figure 1.1.4 Morphological diagram of UHMW-PE[18]

Other types of Polyethene include Ultra Low weight Polyethylene (ULMW-PE), High-Density Cross-Linked Polyethylene (HDCL-PE), Cross-Linked Polyethylene, Very Low-Density Polyethene, and Chlorinated Polyethylene.[11] In this research, we focus on exploring the twisting capabilities of HDPE. HDPE has exhibited twisting characteristics and not much study has been done concerning graphene incorporation and a banded HDPE crystal structure. These concepts will be discussed in the following chapters.

We studied twisting with different weight percentages of graphene induced in HDPE microfibers. Details regarding the synthesis and results with twisting will be discussed in the forthcoming chapters.

1.2 High-Density Polyethylene (HDPE)

As discussed earlier, HDPE is the most used engineering thermoplastic in today's consumer products market. Its low cost and abundance in availability have led to continuous attempts for improvements through intensive research of HDPE to explore its flexibility.

HDPE can be manufactured from translucent milk jugs to colored laundry containers. Compared to other polymers such as PET, HDPE is comparatively easier to recycle, and not degraded over multiple cycles of heat.[19]

Figure 1.2.1 Various HDPE Containers[20]

HDPE composites have proven to find a wide range of applications such as electrical, mechanical, or biomedical. HDPE along with a fraction of additives have proven to enhance its properties. The mechanical and electrical properties, as well as the bio-response of HDPE, are proven to increase with the addition of inorganic particles.[21,22] Numerous studies have previously attempted to investigate the effect of different nanoparticles in HDPE. Nanoparticles such as carbon nanotubes, modified and pristine montmorillonite, and SiO_2 particles were studied by Chrissafis *et al*[23] to enhance the flame retardance and tensile strength character of HDPE.[23,24] Whereas multi-walled Carbon Nanotubes additions have depicted an increase in thermal conductivity and stiffness.[25,26,27]

Several studies have explored graphene nanoparticles as potential fillers and have exhibited a wide range of enhancements in terms of mechanical properties. It is wise to consider graphene as a filler to develop polyethylene composites. However, the quality of graphene matters and the procedure used to synthesize has a crucial role in terms of properties and many more such concerns. Graphene is often functionalized to make it more versatile with properties.

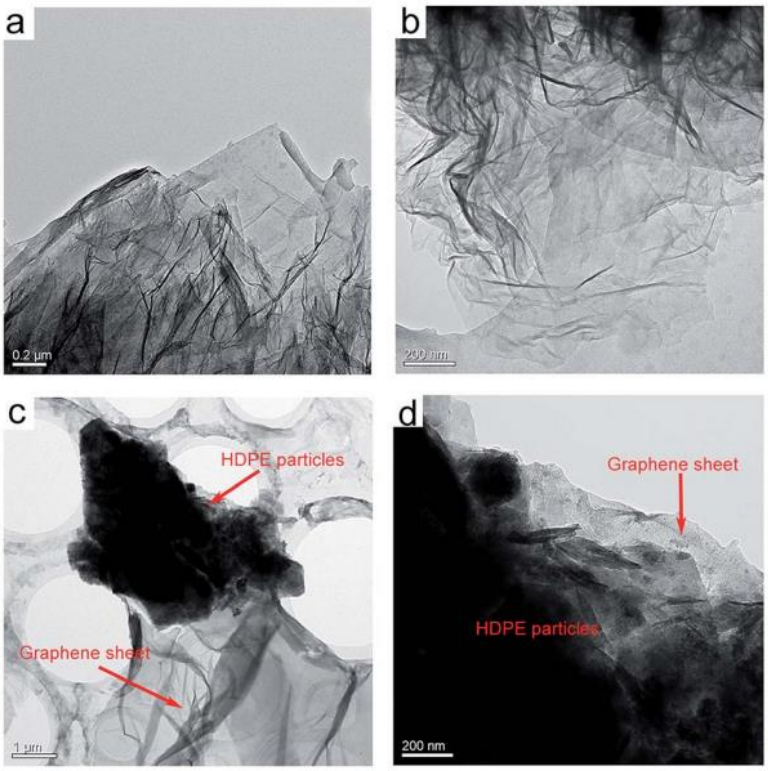

Figure 1.2.3 Transition Electron Microscopy Image of Graphene-HDPE composites[28]

Developing Graphene Oxide (GO)-HDPE composites comes with a lot of complex experimental challenges concerning the infusion of graphene in the polymer matrix, processing techniques, quantitative approximations, and many more. It is very crucial that these concepts are well understood and a design of experiments is developed to obtain desired properties in a composite. Graphene-HDPE composites have been previously developed using melt processing, where yield strength, impact strength, and elongation at break are improved.[28]

1.3 Graphene

Graphene is a single layer of hexagonally structured carbons with sp^2 hybridization[29,30] and has emerged to be one of the biggest scientific interests over the past decade. Graphene can be synthesized using chemical vapor deposition, chemical oxidation of natural graphite, or mechanical cleavage of graphite.[31,32] Graphene can exist in three different structures: pristine graphene, graphene oxide, and reduced graphene oxide. All three forms have distinct properties and are applied very specifically for applications. In this research, we have synthesized graphene oxide following Hummer's method with a few modifications.

The peculiar chemical and physical properties of graphene have paved the way in expanding horizons with its research. Graphene found its way into semiconductors, electronic devices, bio-medical applications composites, and countless more applications. Composites reinforced with graphene pave the way to a vast spectrum of electronic[31,33,34], mechanical[35,36], thermal[37–39], and many more applications. Various attempts have been made to reinforce graphene in polymer to synthesize superior composites and many have succeeded in doing it.

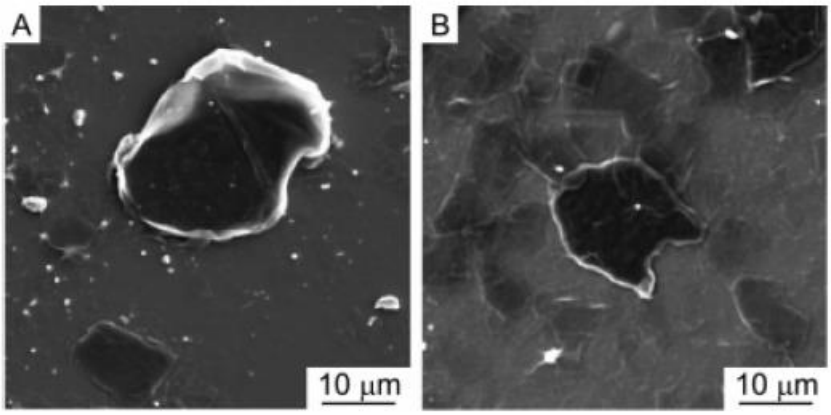

Figure 1.3.1 Scanning Electron Microscopy of GO[40].

Exploring graphene can be interesting, recently, Herrero et al. from the Massachusetts Institute of Technology discovered superconductivity in graphene by introducing a magic angle twist over two sheets of graphene.[41] It was further incorporated into a device to further study. Graphene has over proved to be one of the best fillers for polymer composites over the years indeed surprising how small portions of graphene can bring an exponential change to some of the polymer matrices. These enhancements can depend on how graphene is dispersed inside the polymers. Previous research has proven that graphene incorporations in polymer composites have successfully improved electrical conductivity[42,43], mechanical properties[18], gas permeation[44,45], thermal stability[18,46,47], and many more.

In this research, we reinforce graphene oxide with high-density polyethylene to further study the crystallographic changes influenced by different graphene concentrations.

1.4 Banding

Banding can be defined as the presence of twisted crystallography in a semicrystalline polymer. In other words, it is also a phenomenon by which the spherulites adapsts a preferencial circular arrangement when a semi-crytalline polymer crystallizes from melting temperature. The twisted crystallography denotes a concentric spherulitic arrangement about the radii.[48] The chain-folded lamellae in growth directions have a characteristic rotation by the radii, leading to the formation of concentric circles. These concentric circles can be viewed under a Polarized Optical Microscope (Refer to Figure 1.4.2). The spherulitic crsyatllization takes place when (a) the melt crystallizes with a fibrous habit and (b) the lamellar structures undergo noncrystallograohic branching in a spehrulite.[49] and Figure 1.4.1 shows twisting in a semicrystalline polymer.

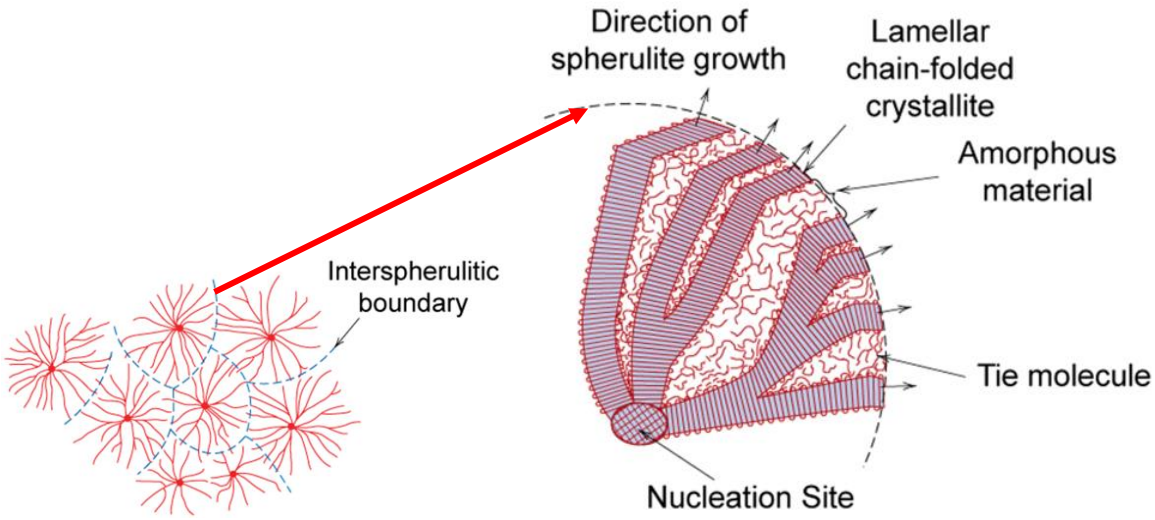

Figure 1.4.1 Twisting in a semicrystalline polymer[50]

Banding was introduced by Keith and Padden during the late 1950s.[51] Keith stated that the systems that induce twisting often have difficulties to undergo homogenous nucleation in the melt.[49] By far, it has been discovered that PE has a unique capability to adapt twisting for its chain macromolecules.[52] It became an area of interest in the early 1950s when PE was still considered a *wonder material*. There is also a bit of uncertainty in terms of radial growth of spherulites and its orgin.[53–55]

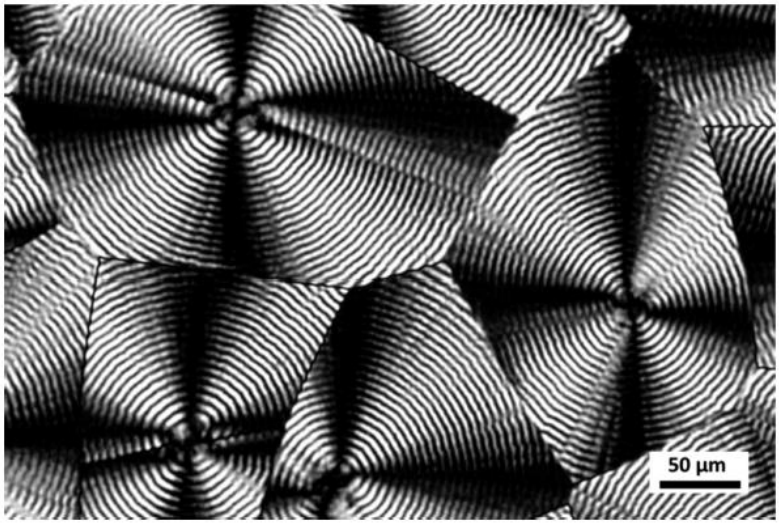

Figure 1.4.2 Twisted spherulites in PE[52]

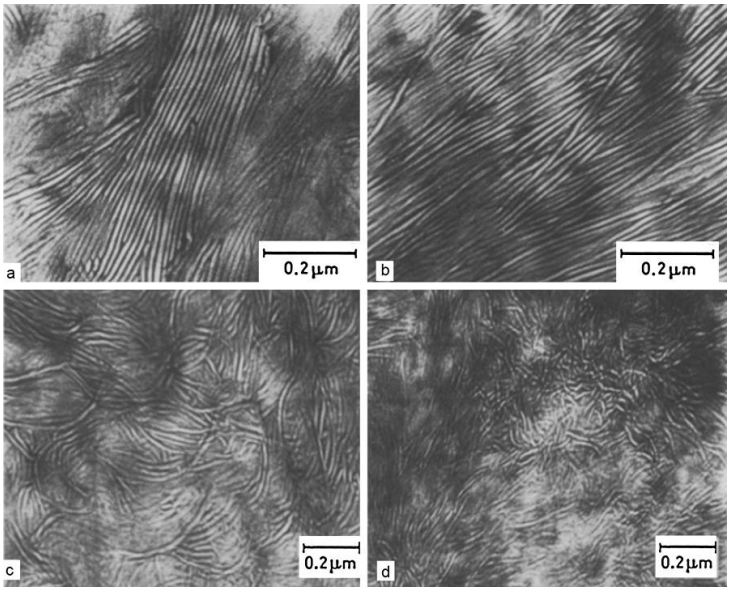

Figure 1.4.3 Twisted spherulites stack observed using a Polarized Optical Microscope

However, not much in detail has been studied or researched about twisting GO-HDPE composites. The literature on this particular topic is also very scarce. This was the major motivation for our research, we wanted to study how graphene incorporations can change/modify the crystallography of HDPE. In the following chapters, we discuss on how we synthesized GO-HDPE microfibers and induced twisting.

Chapter 2: Synthesis of Graphene Oxide High-Density Polyethylene Microfibers (GO-HDPE)

2.1 Methodology

The GO-HDPE microfibers are synthesized using an MC5 Xplore twin-screw extruder or a micro-compounder with a Fiber Line Winder Setup. The HDPE pellets are fed into the extruder and extruded with optimal processing parameters. Once the fibers are extruded, they are stretched to the winder and pulled at a constant speed.

2.1.1 Extruder

The MC5 twin-screw extruder is a vertical extruder with a capacity of 5 ml volume capacity and manufactured by Xplore Instruments[56]. For this research, the HDPE pellets with a melt flow index of 12g/10min (190 C under a 2.16 Kg load) are introduced into the barrel of the extruder using a hopper.

Proper control over temperature and screw speed is very crucial for a successful extrusion. The heating zones in the barrel give good control over temperature, whereas the twin screws provide sufficient torque that contributes to a homogenous mixture of pellets and graphene oxide. The mechanical shear and the thermal energy are responsible for the good mixture of HDPE pellets and GO[57]. The extruder has two sets of dies of dimensions of 0.5 mm and 2 mm. These dies can be used to extrude different thicknesses of fibers as per requirement.

2.1.2 Fiber Winder

The fiber winder is set up in conjunction with the twin screw extruder. The main purpose of the winder is to stretch and elongate the fiber composites extruded. The winder is very crucial in terms of the diameter and length of the fiber, the winding speed and the torque set in the winder decide these factors. The winder unit is also equipped with air cooling for proper function.

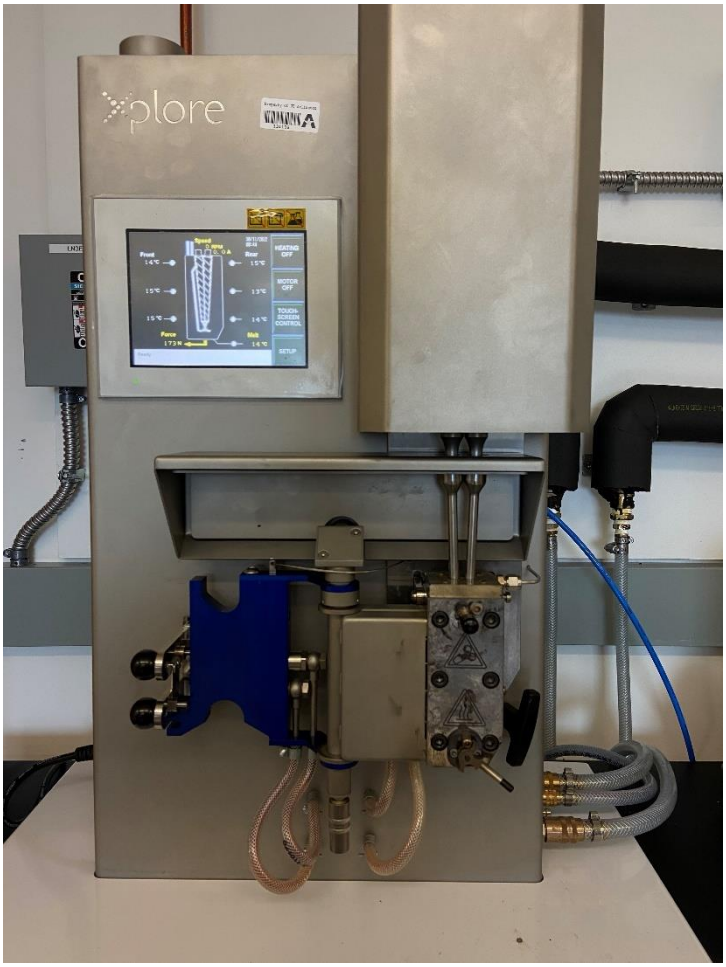

Figure 2.1.1 Xplore Twin Screw Extruder

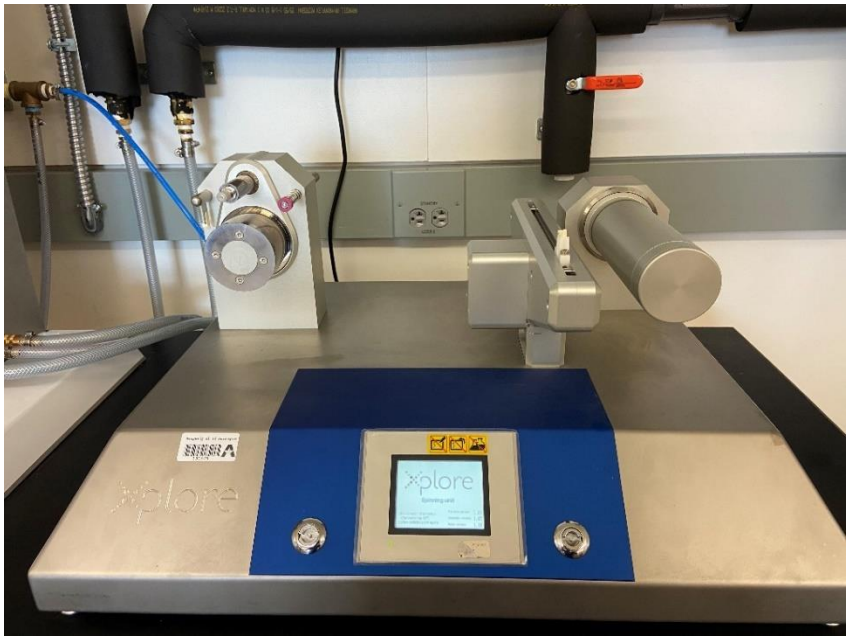

Figure 2.1.2 Xplore Fiber Winder

2.2 Synthesis

Two batches of GO-HDPE fibers were extruded with different weight percentages of GO along with a batch of neat HDPE fibers. The following parameters were followed for the extrusion process.

Table 2.1.1 Extrusion Parameters

Parameters	Value
Operating temperature	140º C
Operating RPM	80
Force generated during processing	900 N
Extruding RPM	50
Winder Speed	13.5 mm/min
Torque	30

Table 2.1.2 Batches of fibers produced

Sample	wt. % GO	Average Diameter (µm)
Neat	0	49 ± 2
GO-HDPE	0.0025	50 ± 2
GO-HDPE	0.0050	50 ± 2

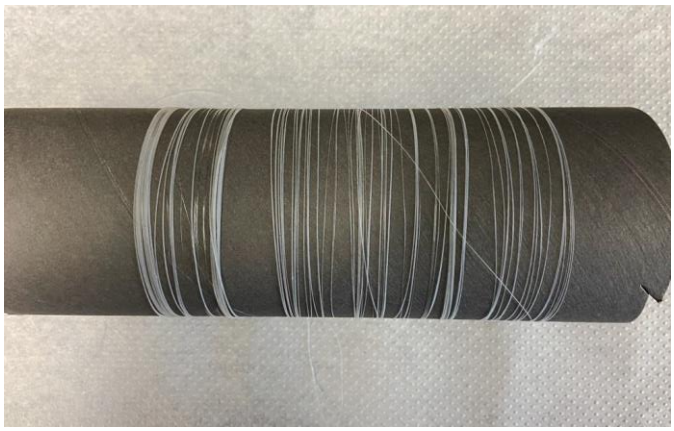

Figure 2.1.3 Neat HDPE Fiber

Chapter 3: Characterization of the Microfibers

3.1 Polarized Optical Microscope Images

The Optical Microscope utilizes visible light followed by a system of lenses to magnify samples.[58] These microscopes have evolved over the years and are more complex in architecture. They help researchers view micron-range structures, investigate surface profiles, and even concentrate on a cross-section desired.[59] To use an optical microscope efficiently one should understand concepts such as magnification, resolution, numerical aperture, illumination and focusing very well. To characterize the HDPE fiber composites, a polarizing filter was attcahed to the optical microscope. A Zeiss Axioscope 5 Optical Microscope was used to characterise the fibers (refer to figure 4.1.1). This microscope comes with N-Achroplan 10x, 40x, and 100x objective lenses. The microscope is equipped with an Abbe condenser 0.9/1.25NA and uses a 10W transmitted white LED for illuminations. The microscope also comes with an Axiom 209 colour microscope camera capable of generating images at 4k resolution.[60]

Figure 3.1.1 Zeiss Axioscpe 5 Optical Microscope

The HDPE fibers were held in between the cross polarizers of the Polarized Optical Microscope. The fibers were observed in parallel, at a 45 º rotated angle, and perpendicular to

the analyzer. When the fibers are rotated at 45º, the fibers appear brighter. The GO-HDPE composite fibers (0.0025 wt. % and 0.005 wt.%) exhibit strong birefringence. The birefringence also states that the HDPE crystals adopt a preferential orientation along the long axis of fibers.61 These could also be due to the directional shear forces during the extrusion process. The images of the fibers characterized are given below.

a) Neat HDPE

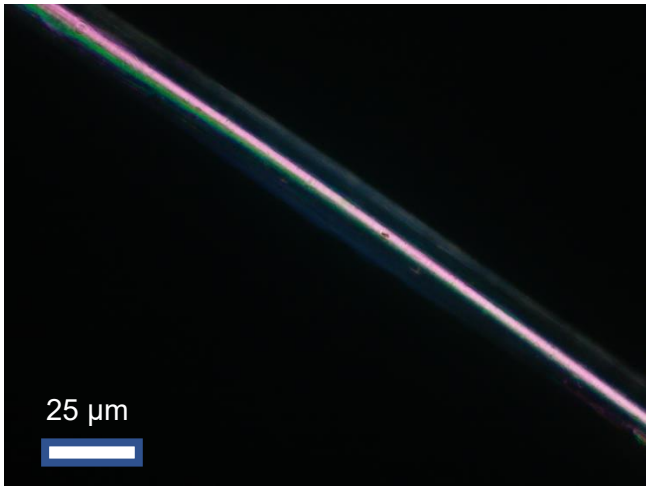

Figure 3.1.2 Neat HDPE Fibers at 45º

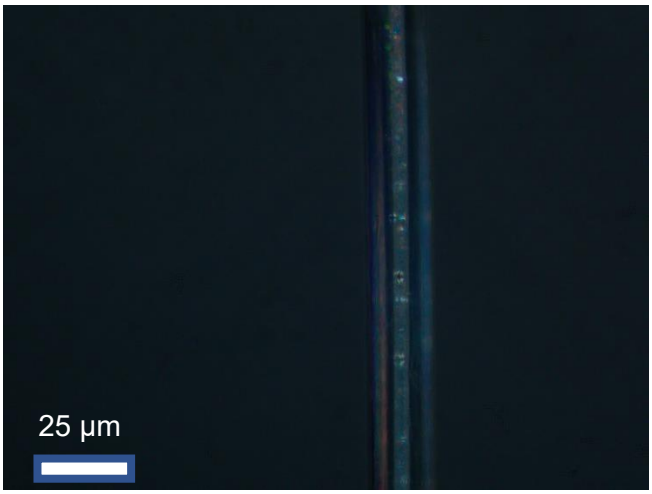

Figure 3.1.3 Neat HDPE Fibers at perpendicular orientation

b) HDPE + 0.0025 wt.% GO

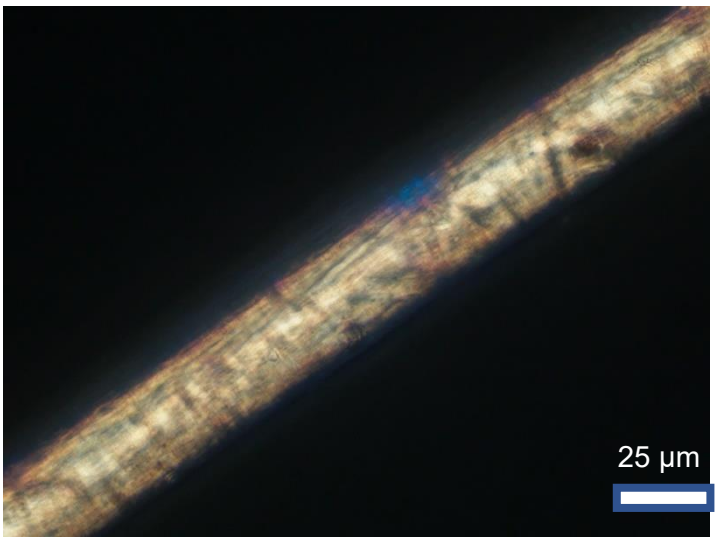

Figure 3.1.4 HDPE + 0.0025 wt.% GO fiber at 45 º

Figure 3.1.5 HDPE + 0.0025 wt.% GO fiber in perpendicular orientation

c) HDPE + 0.005 wt.% GO

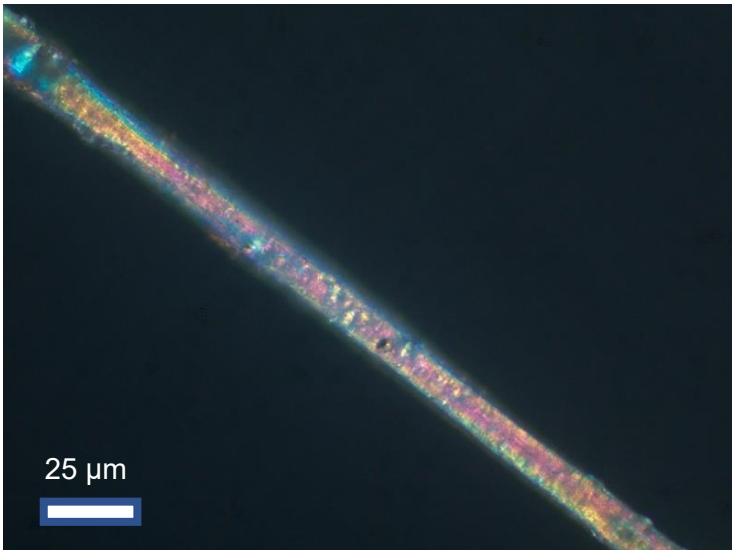

Figure 3.1.6 HDPE + 0.005 wt.% GO fiber at 45

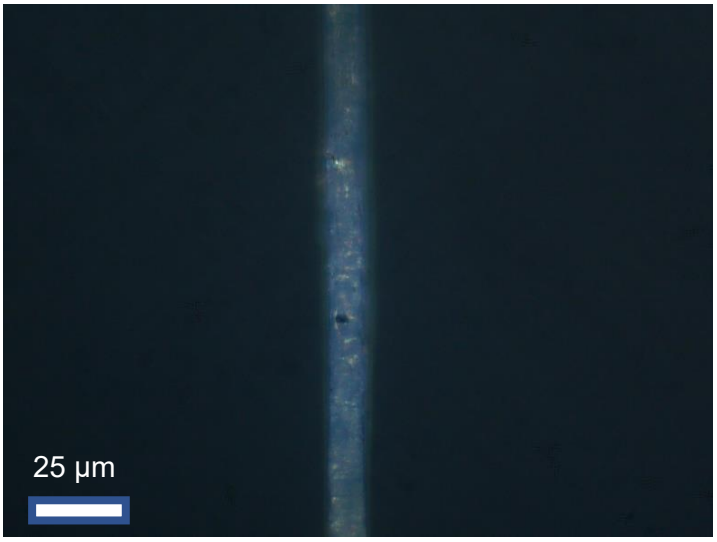

Figure 3.1.7 HDPE + 0.005 wt.% GO fiber in perpendicular orientation

When the fibers are rotated at 45º, the fibers appear brighter. The GO-HDPE composite fibers (0.0025 wt. % and 0.005 wt.%) exhibit strong birefringence. The birefringence also states that the HDPE crystals adopt a preferential orientation along the long axis of fibers.[61] These could also be due to the directional shear forces expereinced uring the extrusion process.

Recrystallization

The fibers did not depict any evidence of twisting when observed with an optical microscope right after extrusion. Therefore, we decided to recrystallize the fibers between 220 and 110º C to form thick films down to approximately 5µm. Firstly, the fibers were held in between two glass slides and heated to a temperature of 220 ºC for 60 seconds and pressure was applied to the samples to spread the melt. The film sandwiches between the glass slides were quickly cooled at a temperature of 110 ºC for five seconds followed by cooling at room temperature.

Table 3.1 Recrystallization Parameters

Parameters	**Value**
Melting Temperature	220 ºC
Melting Time	60 seconds
Quenching Temperature	110 ºC
Quenching Time	5 seconds
Film Thickness	5 µm

a) Neat HDPE Fiber

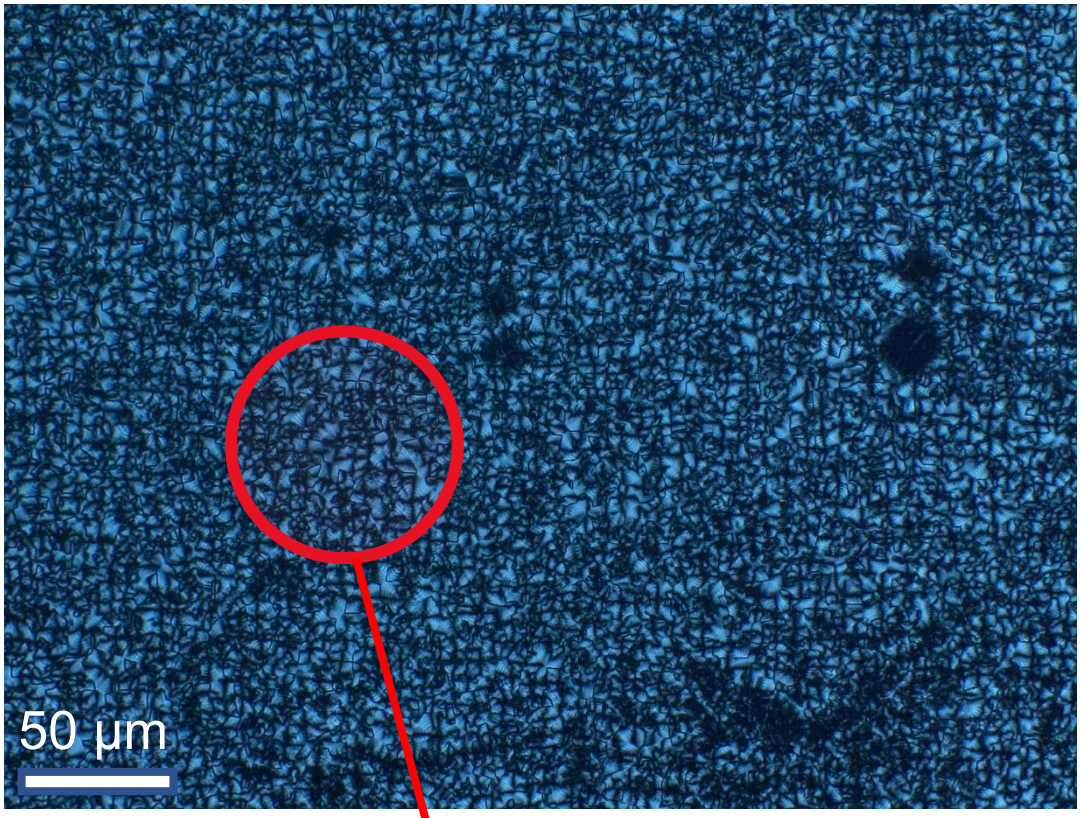

Figure 3.2.1 POM Images of Neat HDPE Fibers

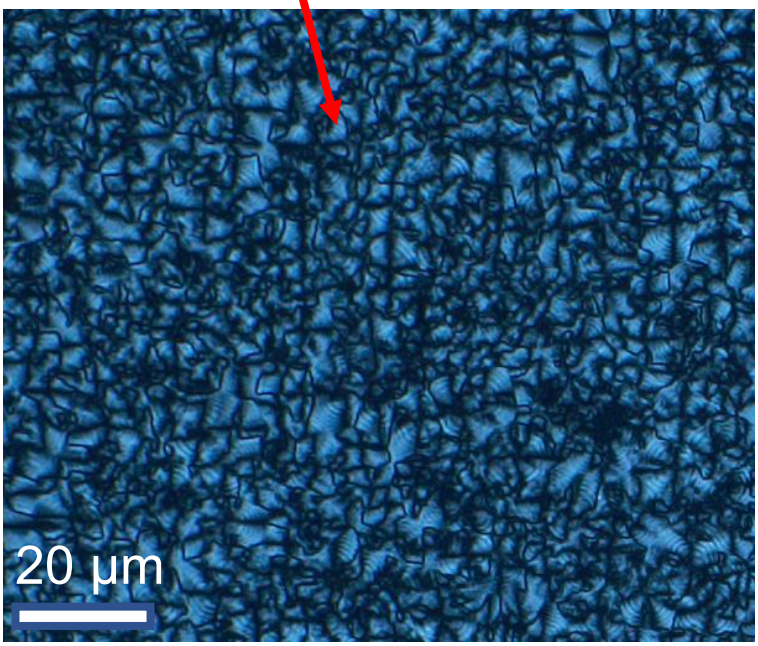

Figure 3.2.2 Magnified POM Images of Neat HDPE Fibers

b) HDPE + 0.0025 wt.% GO

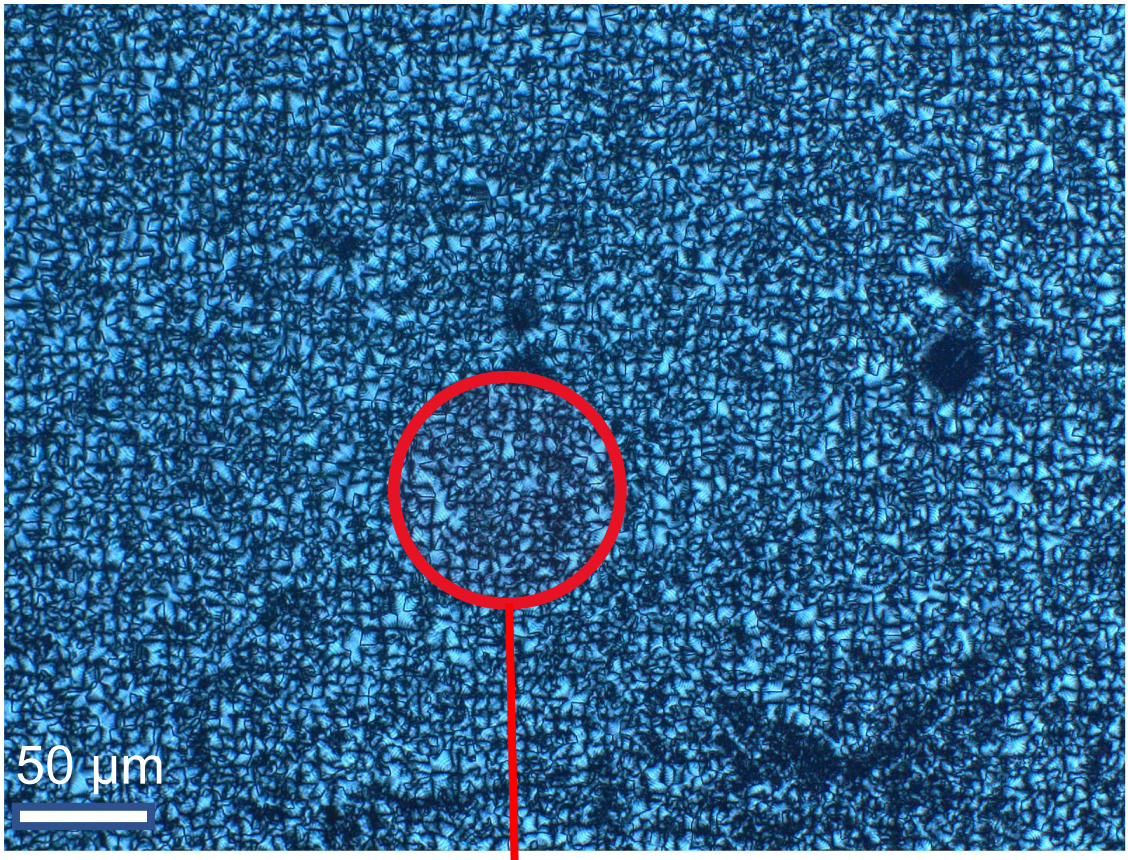

Figure 3.2.3 POM Image of HDPE + 0.0025 wt.% GO

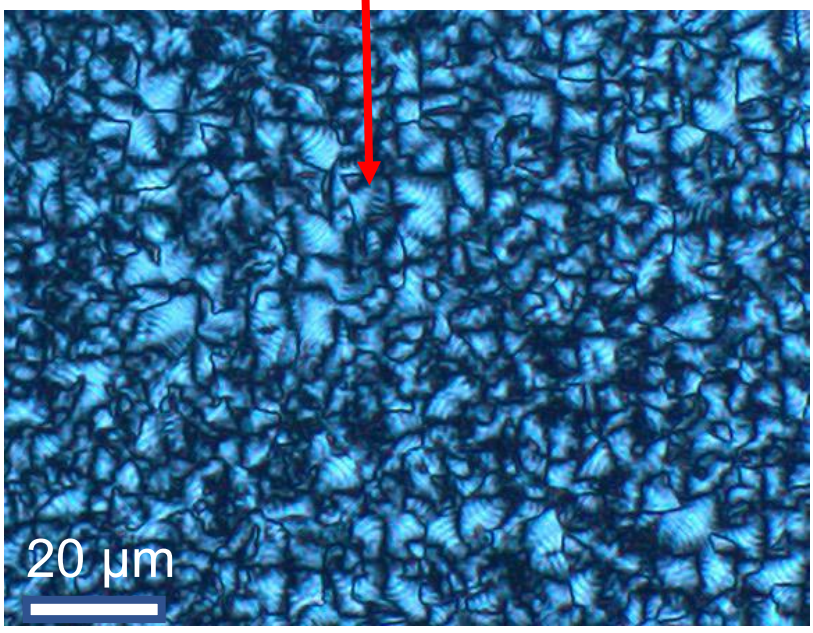

Figure 3.2.4 Magnified POM Image of HDPE + 0.0025 wt.% G

c) HDPE + 0.0005 wt.% GO

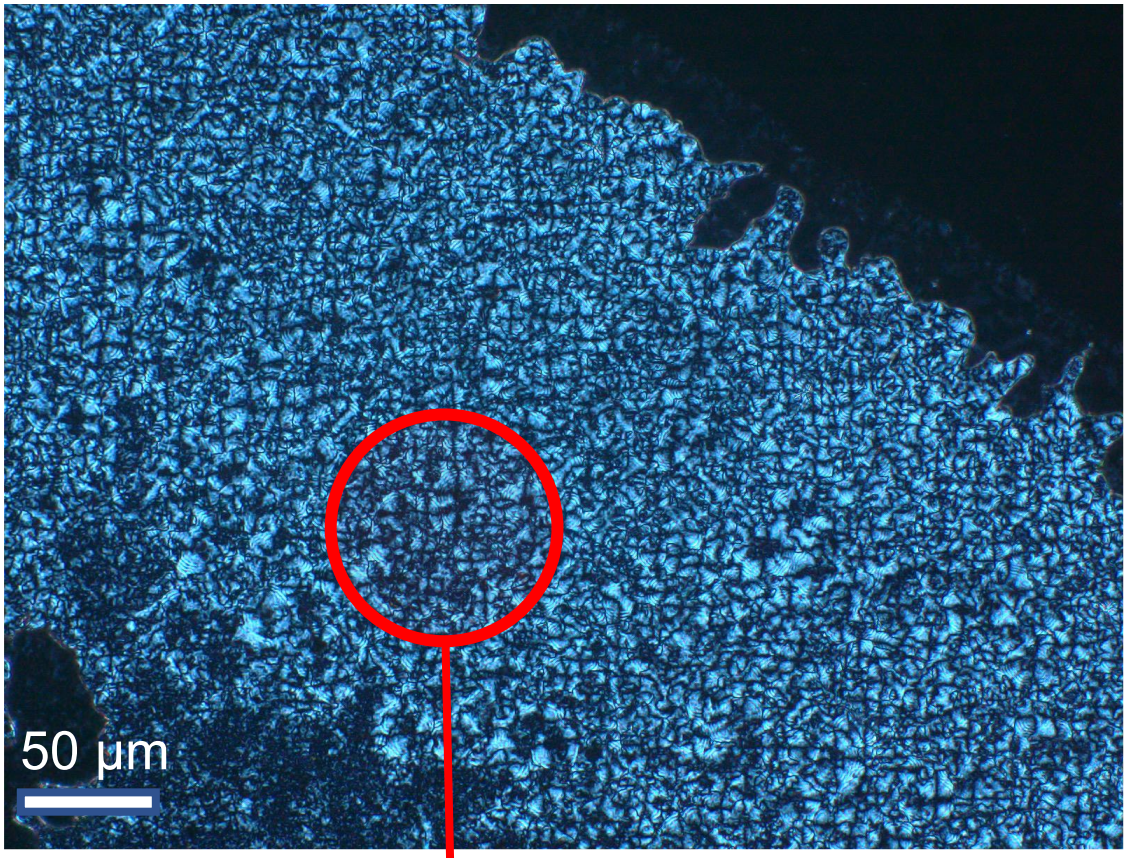

Figure 3.2.5 POM image of HDPE + 0.0005 wt.% GO

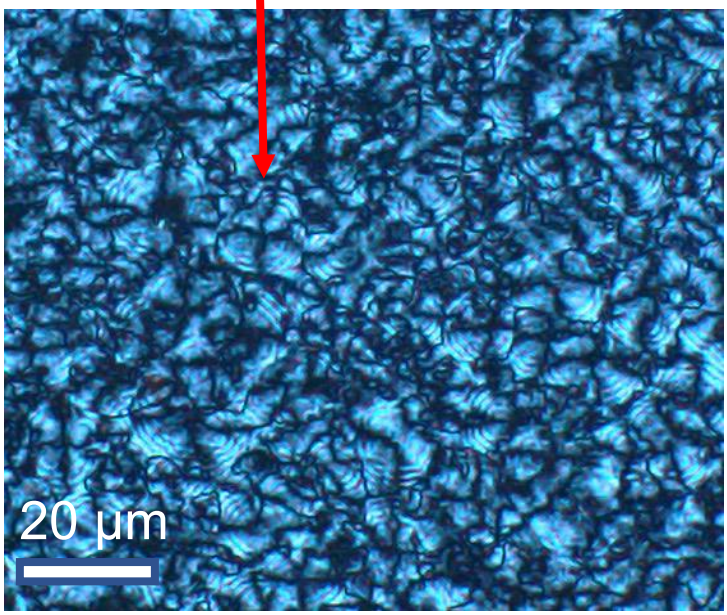

Figure 3.2.6 POM image of HDPE + 0.0005 wt.% GO

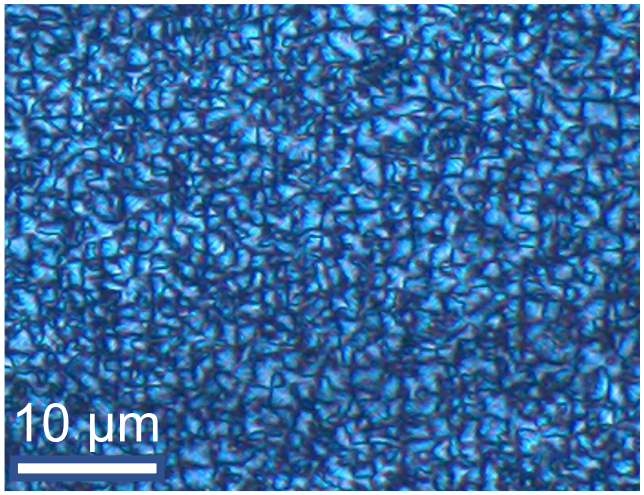

Neat HDPE fibers

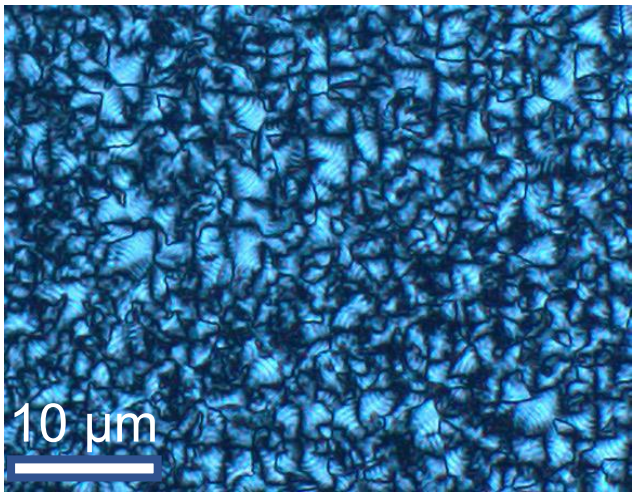

HDPE + 0.0025 wt.% GO

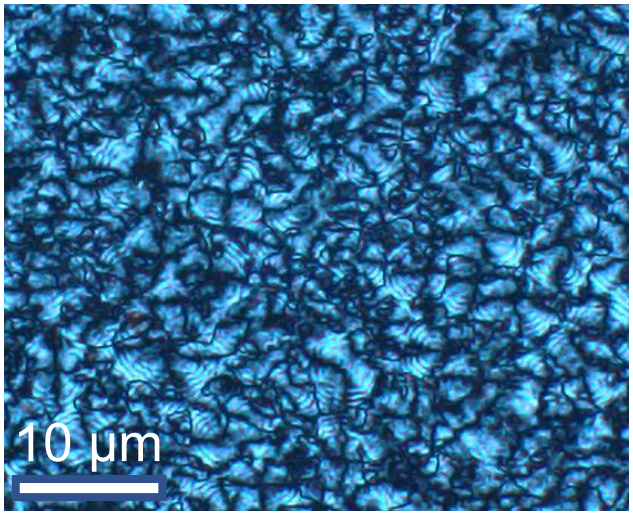

HDPE + 0.005 WT.% GO

Figure 3.2.7 Comparison of three batches

Figure 3.2.4 compares the three batches and helps us in identifying the batch with the most twisting and the one with least.

The neat HDPE fibers, after recrystallization, shows good evidence of crystal twisting with good nucleation density. From Figure 3.2.1, the densely packed spherulitic arrangement is evident and indicates extensive twisting. In the case of HDPE + 0.005 wt.% GO it has been observed that the extent of twisting has been lower (Refer to Figure 3.2.2), and the spherulitic arrangement is lesser dense than HDPE + 0.0025 wt.% GO and the nucleation density is comparatively smaller. This is possibly due to the higher incorporations of GO. In HDPE + 0.0025 wt.% GO, we could observe better nucleation density, spherulitic arrangement and a good extent of twisting.

It has been observed that the incorporations of GO have influenced the nucleation density of the GO-HDPE fibers where the increased loading of GO exhibits a hindrance in nucleation density but may or may not interfere with crystal twisting. In the case of the GO-HDPE fiber composites with 0.005wt.% GO (refer to Figure 3.2.3), the nucleation density, and spherulitic intensity can be observed to be lesser with an average spherulite size of 25μm than the case of 0.0025 wt.% GO (refer to Figure 3.2.2). These images stand as evidence for the observation related to the GO loading and nucleation in HDPE[61].

3.3 X-RAY DIFFRACTION

XRD is a powerful analytical technique to investigate the atomic structures of solid materials. XRD spectroscopy is widely used for understanding phase identification, crystal size and many more.[62,63] XRD works on the basic principles of Bragg's Law (Refer to Equation 1) where the incident X-ray with an angle of incidence 'Ɵ' on a crystal surface produces the same angle of scattering 'Ɵ'. When 'd', the path difference is equal to a constant 'n', a constructive intereference occurs.[64,65]

$$n(\lambda) = 2dsin(\theta) \quad (1)$$

An X-ray instrument contains three main components: an X-ray source, a sample holder and an XRD detector[66]. XRD is usually very quick with producing results and accurate with identifying unknown materials. For our study, we used a Philips Panalytical X'Pert XRD to analyse the thin films after recrystallization.

Figure 3.3.1 Philips Pananalytical XRD[67]

Following are the results of the analysis performed for the two GO-HDPE fiber composites (0.0025 and 0.005 wt. % GO).

a) HDPE + 0.0025 wt. % GO

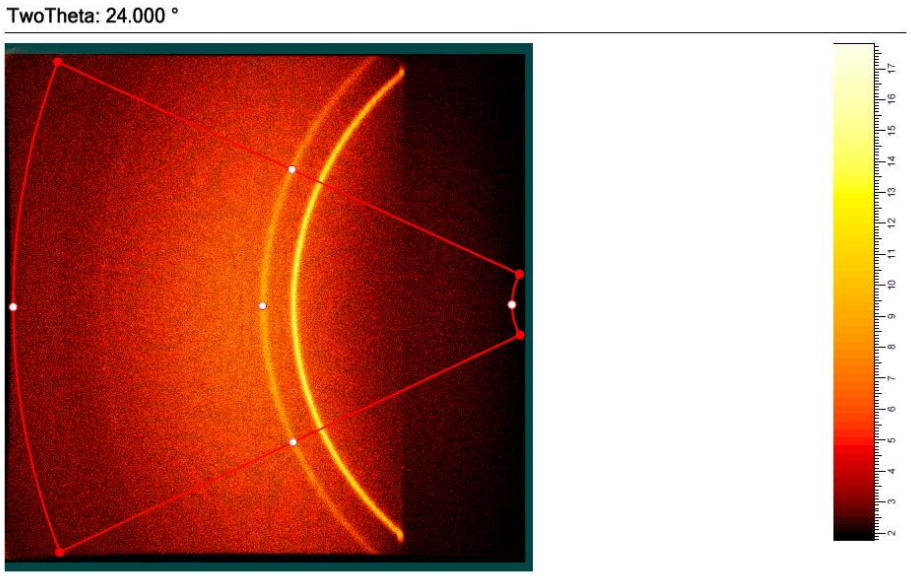

Figure 3.3.2 2D X-ray Diffraction Pattern for HDPE + 0.0025 wt.% GO at a scale of intensity per hundred counts

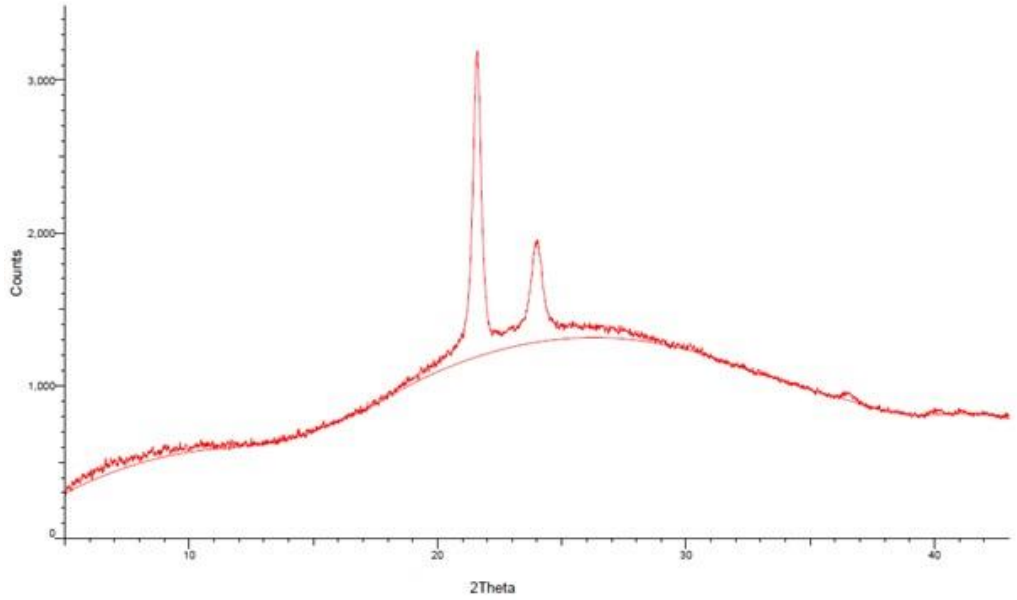

Figure 3.3.3 X-ray peaks for HDPE + 0.0025 wt. % GO

b) HDPE + 0.005 wt. % GO

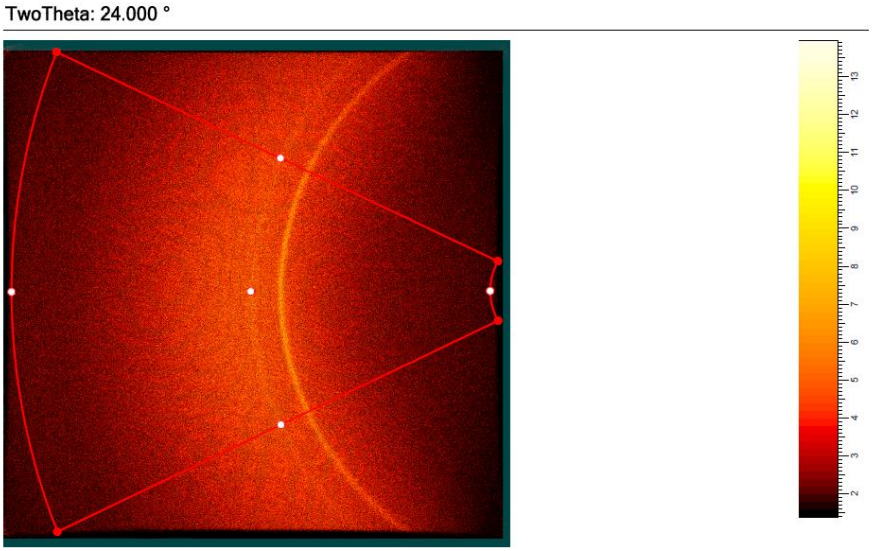

Figure 3.3.4 2D X-ray Diffraction Pattern for HDPE + 0.005 wt.% GO at a scale of intensity per hundred counts

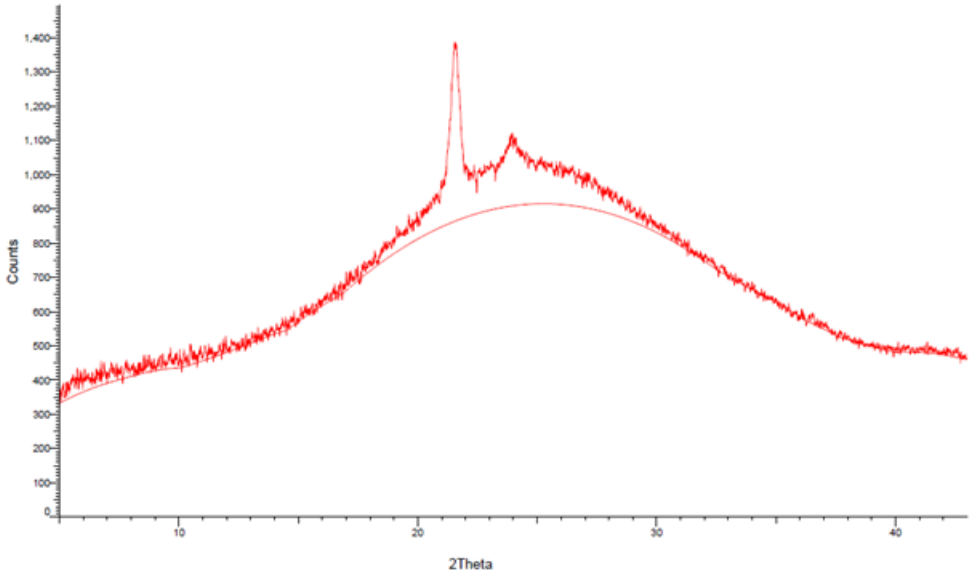

Figure 3.3.5 X-ray peaks for HDPE + 0.005 wt.% GO

The XRD results suggest that the x-ray intensity is observed to be twice in HDPE + 0.0025 wt.% GO than HDPE + 0.005 wt.% GO (Refer to Figures 3.3.4 and 3.3.2). The diffractions patterns are analyzed at scale of intensity per 100 hundred counts. This is possible because of the denser spherulitic concentration in the HDPE + 0.0025 wt.% GO and the stronger interference of GO and HDPE. With a higher concentration of GO in HDPE + 0.005 wt.% GO fibers, there has been a hindrance in the nucleation which has had an impact on spherulitic growth. The peaks from the above graphs also aligns well with the literature reviewed. Sharp rings indexed to planes (110), (200), and (020) are strongly evident for both the GO-HDPE fiber composites.

3.4 Scanning Electron Microscopy

A Scanning Electron Microscope (SEM) is an accurate imaging technique to understand and investigate a sample's composition and topography. SEM uses a stream of electrons over the surface of a sample to produce a highly magnified image.[68] An electron gun is used to produce a beam of electrons which concentrates on the sample, followed by ejections of secondary electrons from the sample.[69] Detectors collect these outputs and transfer signals which further create a magnified image. SEM can be used to investigate the sample's composition and topography in detail.

Figure 3.4.1 Hitachi SEM[70]

We have used a HITACHI Scanning Electron Microscope SU3800 to analyze the HDPE + 0.0025 wt. % GO fiber composite. The SEM comes with a secondary electron resolution of 15.0 nm and 4.0 nm in the backscattered electron resolution.[70]

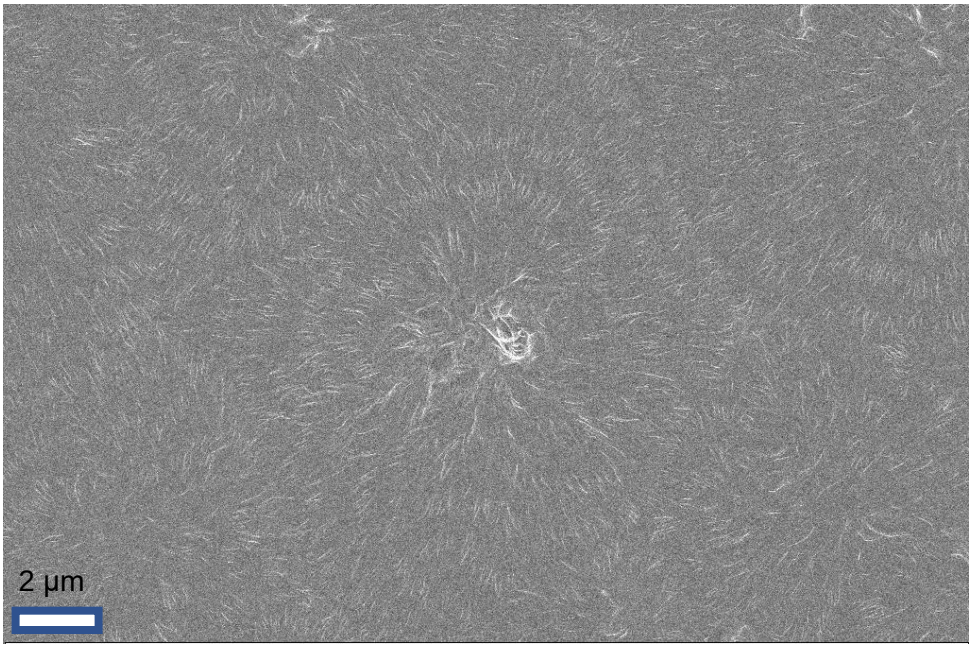

Figure 3.4.2 Scanning Electron Microscopy Image of HDPE + 0.0025 wt.% GO fiber composite

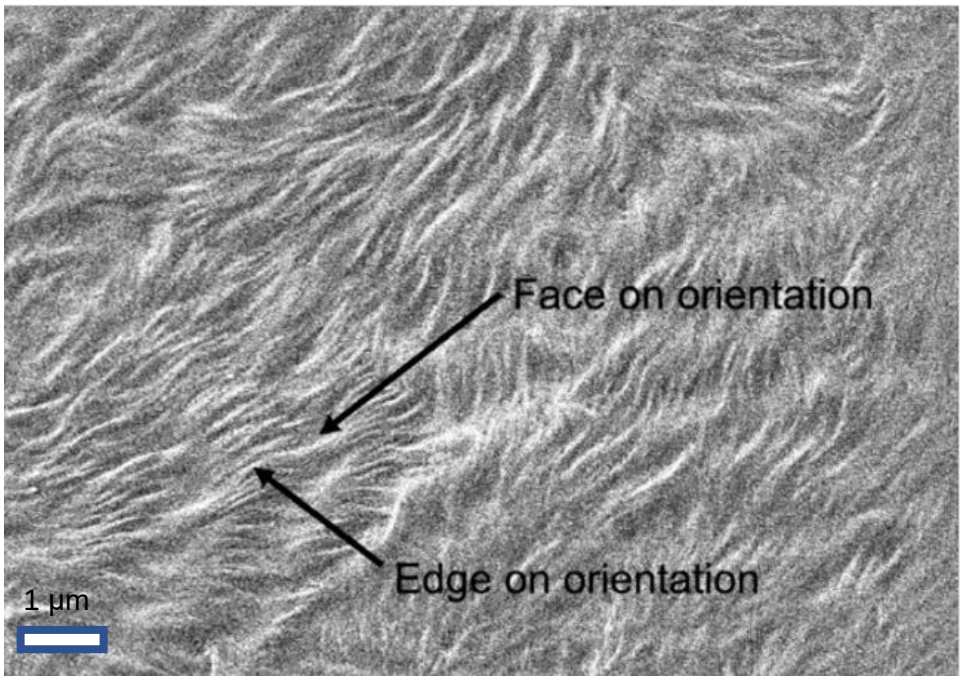

Figure 3.4.3 Scanning Electron Microscopy Images of Face-on and Edge-on orientation in HDPE+ 0.0025 wt.% GO

SEM images suggest that there are alternating face-on and edge-on orientations of lamellae as they twist. This orientation has its origin in the process of recrystallization of the fibers at temperatures above the melting point. Figure 4.4.2 also indicates a certain definite flow which proves there has been good homogenous mixing of GO with the pellets.

Conclusion

Two batches of GO-HDPE and neat HDPE fibers were produced in the range of 40-50 microns using a twin-screw extruder after carefully deducing optimal extrusion parameters. The fibers were twisted by recrystallizing them into thick films by holding the fibers holding it between glass slides at 220º C and 110º C. The films were later cooled to room temperature.

The three samples; neat HDPE fibers, HDPE + 0.0025 wt.% GO and HDPE + 0.005 wt.% GO was characterized using Polarized Optical Microscope, X-ray Diffraction and Scanning Electron Microscopy. Twisting was very evident from the images from Polarized Optical Microscope; however, the extent of twisting seems to hinder higher incorporations of GO. Sample HDPE + 0.005 wt.% GO exhibited a lower concentration of lamellae and spherulitic growth when compared with HDPE + 0.0025 wt.% GO. Increasing the concentration of GO might influence nucleation growth.

The samples HDPE + 0.0025 wt.% GO and HDPE + 0.005 wt.% GO was examined under XRD. X-Ray Diffraction spectroscopy analysis confirms that the HDPE + 0.0025 wt.% GO fiber composite seems to have a higher intensity of lamellae packing than that of HDPE + 0.005 wt.% GO.

Scanning electron microscopy imaging was performed for HDPE + 0.0025 wt.% GO suggests that there is a presence of alternating bands of edge-on and face-on orientation of lamellae present in the fiber composite. These orientations have originated due to the influence of variance of temperature during the recrystallization process.

It is concluded that higher GO incorporations have an influence on spherulitic growth which slows the nucleation. However, the results also suggest that the fibers could find their application in the design of multifunctional composites such as flexible composites.

This work was published and presented at the American Society for Composites (ASC) 37th Annual Technical Conference held at the University of Arizona in September 2022.

References

(1) Geyer, R.; Jambeck, J. R.; Law, K. L. Production, Use, and Fate of All Plastics Ever Made. *Sci. Adv.* **2017**, *3* (7). https://doi.org/10.1126/SCIADV.1700782/SUPPL_FILE/1700782_SM.PDF.

(2) Ucankus, G.; Ercan, M.; Uzunoglu, D.; Culha, M. Methods for Preparation of Nanocomposites in Environmental Remediation. *New Polym. Nanocomposites Environ. Remediat.* **2018**, 1–28. https://doi.org/10.1016/B978-0-12-811033-1.00001-9.

(3) Manjula, B.; Reddy, A. B.; Sadiku, E. R.; Sivanjineyulu, V.; Molelekwa, G. F.; Jayaramudu, J.; Raj Kumar, K. Use of Polyolefins in Hygienic Applications. *Polyolefin Fibres Struct. Prop. Ind. Appl. Second Ed.* **2017**, 539–560. https://doi.org/10.1016/B978-0-08-101132-4.00018-7.

(4) Basmage, O. M.; Hashmi, M. S. J. Plastic Products in Hospitals and Healthcare Systems. *Encycl. Renew. Sustain. Mater.* **2020**, 648–657. https://doi.org/10.1016/B978-0-12-803581-8.11303-7.

(5) Heitkemper, M.; Dasi, L. P. Polymeric Heart Valves. *Princ. Hear. Valve Eng.* **2019**, 343–359. https://doi.org/10.1016/B978-0-12-814661-3.00013-7.

(6) Sastri, V. R. Commodity Thermoplastics: Polyvinyl Chloride, Polyolefins, Cycloolefins and Polystyrene. *Plast. Med. Devices* **2022**, 113–166. https://doi.org/10.1016/B978-0-323-85126-8.00002-3.

(7) Shinohara, K. ichi; Yanagisawa, M.; Makida, Y. Direct Observation of Long-Chain Branches in a Low-Density Polyethylene. *Sci. Reports 2019 91* **2019**, *9* (1), 1–5. https://doi.org/10.1038/s41598-019-46035-9.

(8) *Polyethylene (PE) - Properties, Uses & Application.* https://omnexus.specialchem.com/selection-guide/polyethylene-plastic (accessed 2022-12-08).

(9) Selke, S. E.; Hernandez, R. J. Packaging: Polymers in Flexible Packaging. *Encycl. Mater. Sci. Technol.* **2001**, 6652–6656. https://doi.org/10.1016/B0-08-043152-6/01176-1.

(10) Pham, N. T. H. Characterization of Low-Density Polyethylene and LDPE-Based/Ethylene-Vinyl Acetate with Medium Content of Vinyl Acetate. *Polymers (Basel).* **2021**, *13* (14). https://doi.org/10.3390/POLYM13142352.

(11) Rohani Shirvan, A.; Nouri, A.; Wen, C. Structural Polymer Biomaterials. *Struct. Biomater. Prop. Charact. Sel.* **2021**, 395–439. https://doi.org/10.1016/B978-0-12-818831-6.00010-0.

(12) Goswami, T. K.; Mangaraj, S. Advances in Polymeric Materials for Modified Atmosphere Packaging (MAP). *Multifunct. Nanoreinforced Polym. Food Packag.* **2011**, 163–242. https://doi.org/10.1533/9780857092786.1.163.

(13) Sastri, V. R. Commodity Thermoplastics: Polyvinyl Chloride, Polyolefins, Cycloolefins and Polystyrene. *Plast. Med. Devices* **2022**, 113–166. https://doi.org/10.1016/B978-0-323-85126-8.00002-3.

(14) Emblem, A. Plastics Properties for Packaging Materials. *Packag. Technol.* **2012**, 287–309. https://doi.org/10.1533/9780857095701.2.287.

(15) Selke, S. E.; Hernandez, R. J. Packaging: Polymers for Containers. *Encycl. Mater. Sci. Technol.* **2001**, 6646–6652. https://doi.org/10.1016/B0-08-043152-6/01175-X.

(16) Van Der Werff, H.; Heisserer, U. High-Performance Ballistic Fibers: Ultra-High Molecular Weight Polyethylene (UHMWPE). *Adv. Fibrous Compos. Mater. Ballist. Prot.* **2016**, 71–107. https://doi.org/10.1016/B978-1-78242-461-1.00003-0.

(17) Shen, F. W. Ultrahigh-Molecular-Weight Polyethylene (UHMWPE) in Joint Replacement. *Biomed. Polym.* **2007**, 141–173. https://doi.org/10.1533/9781845693640.141.

(18) Rafiee, M. A.; Rafiee, J.; Wang, Z.; Song, H.; Yu, Z. Z.; Koratkar, N. Enhanced Mechanical Properties of Nanocomposites at Low Graphene Content. *ACS Nano* **2009**, *3* (12), 3884–3890. https://doi.org/10.1021/NN9010472.

(19) Spencer, D. B. Recycling—Household Waste. *Encycl. Mater. Sci. Technol.* **2005**, 1–9. https://doi.org/10.1016/B0-08-043152-6/02051-9.

(20) Fink, J. K. Compatibilization. *React. Polym. Fundam. Appl.* **2013**, 373–409. https://doi.org/10.1016/B978-1-4557-3149-7.00016-4.

(21) Fouad, H.; Elleithy, R.; Al-Zahrani, S. M.; Ali, M. A. haj. Characterization and Processing of High Density Polyethylene/Carbon Nano-Composites. *Mater. Des.* **2011**, *32* (4), 1974–1980. https://doi.org/10.1016/J.MATDES.2010.11.066.

(22) Dong, Q.; Zheng, Q.; Du, M.; Zhang, M. Temperature-Dependence of Dynamic Rheological Properties for High-Density Polyethylene Filled with Graphite.

(23) Chrissafis, K.; Paraskevopoulos, K. M.; Tsiaoussis, I.; Bikiaris, D. Comparative Study of the Effect of Different Nanoparticles on the Mechanical Properties, Permeability, and Thermal Degradation Mechanism of HDPE. *J Appl Polym Sci* **2009**, *114*, 1606–1618. https://doi.org/10.1002/app.30750.

(24) Wang, K. H.; Koo, C. M.; Chung, I. J. Physical Properties of Polyethylene/Silicate Nanocomposite Blown Films. *J. Appl. Polym. Sci.* **2003**, *89* (8), 2131–2136. https://doi.org/10.1002/APP.12358.

(25) Wu, F.; He, X.; Zeng, Y.; Cheng, H. M. Thermal Transport Enhancement of Multi-Walled Carbon Nanotubes/ High-Density Polyethylene Composites. *Appl. Phys. A 2006 851* **2006**, *85* (1), 25–28. https://doi.org/10.1007/S00339-006-3649-2.

(26) Trujillo, M.; Arnal, M. L.; Müller, A. J.; Laredo, E.; Bredeau, S.; Bonduel, D.; Dubois, P. Thermal and Morphological Characterization of Nanocomposites Prepared by In-Situ Polymerization of High-Density Polyethylene on Carbon Nanotubes. *Macromolecules* **2007**, *40* (17), 6268–6276. https://doi.org/10.1021/MA071025M/ASSET/IMAGES/LARGE/MA071025MF00009.JPEG.

(27) Osman, M. A.; Rupp, J. E. P.; Suter, U. W. Gas Permeation Properties of Polyethylene-Layered Silicate Nanocomposites. *J. Mater. Chem.* **2005**, *15* (12), 1298–1304. https://doi.org/10.1039/B417673A.

(28) Wei, P.; Bai, S. Fabrication of a High-Density Polyethylene/Graphene Composite with High Exfoliation and High Mechanical Performance via Solid-State Shear Milling. *RSC Adv.* **2015**, *5* (114), 93697–93705. https://doi.org/10.1039/c5ra21271e.

(29) Inagaki, M.; Kang, F.; Toyoda, M.; Konno, H. Graphene: Synthesis and Preparation. *Adv. Mater. Sci. Eng. Carbon* **2014**, 41–65. https://doi.org/10.1016/B978-0-12-407789-8.00003-X.

(30) Chen, K.; Tang, X.; Jia, B.; Chao, C.; Wei, Y.; Hou, J.; Dong, L.; Deng, X.; Xiao, T. H.; Goda, K.; Guo, L. Graphene Oxide Bulk Material Reinforced by Heterophase Platelets with Multiscale Interface Crosslinking. *Nat. Mater. 2022 2110* **2022**, *21* (10), 1121–1129. https://doi.org/10.1038/s41563-022-01292-4.

(31) Novoselov, K. S.; Geim, A. K.; Morozov, S. V.; Jiang, D.; Katsnelson, M. I.; Grigorieva, I. V.; Dubonos, S. V.; Firsov, A. A. Two-Dimensional Gas of Massless Dirac Fermions in Graphene. *Nature* **2005**, *438* (7065), 197–200. https://doi.org/10.1038/NATURE04233.

(32) Novoselov, K. S.; Geim, A. K.; Morozov, S. V.; Jiang, D.; Katsnelson, M. I.; Grigorieva, I. V.; Dubonos, S. V.; Firsov, A. A. Two-Dimensional Gas of Massless Dirac Fermions in Graphene. *Nat. 2005 4387065* **2005**, *438* (7065), 197–200. https://doi.org/10.1038/nature04233.

(33) Novoselov, K. S.; Geim, A. K.; Morozov, S. V.; Jiang, D.; Zhang, Y.; Dubonos, S. V.; Grigorieva, I. V.; Firsov, A. A. Electric Field in Atomically Thin Carbon Films. *Science (80-.).* **2004**, *306* (5696), 666–669. https://doi.org/10.1126/SCIENCE.1102896/SUPPL_FILE/NOVOSELOV.SOM.PDF.

(34) Zhang, Y.; Tan, Y. W.; Stormer, H. L.; Kim, P. Experimental Observation of the Quantum Hall Effect and Berry's Phase in Graphene. *Nat. 2005 4387065* **2005**, *438* (7065), 201–204. https://doi.org/10.1038/nature04235.

(35) Zhao, X.; Zhang, Q.; Chen, D.; Lu, P. Enhanced Mechanical Properties of Graphene-Based Polyvinyl Alcohol Composites. *Macromolecules* **2010**, *43* (5), 2357–2363. https://doi.org/10.1021/ma902862u.

(36) Lee, C.; Wei, X.; Kysar, J. W.; Hone, J. Measurement of the Elastic Properties and Intrinsic Strength of Monolayer Graphene. *Science* **2008**, *321* (5887), 385–388. https://doi.org/10.1126/SCIENCE.1157996.

(37) Balandin, A. A. Thermal Properties of Graphene and Nanostructured Carbon Materials. *Nat. Mater.* **2011**, *10* (8), 569–581. https://doi.org/10.1038/nmat3064.

(38) Balandin, A. A.; Ghosh, S.; Bao, W.; Calizo, I.; Teweldebrhan, D.; Miao, F.; Lau, C. N. Superior Thermal Conductivity of Single-Layer Graphene. *Nano Lett.* **2008**, *8* (3), 902–907. https://doi.org/10.1021/NL0731872.

(39) Goli, P.; Ning, H.; Li, X.; Lu, C. Y.; Novoselov, K. S.; Balandin, A. A. Thermal Properties of Graphene-Copper-Graphene Heterogeneous Films. *Nano Lett.* **2014**, *14* (3), 1497–1503. https://doi.org/10.1021/nl404719n.

(40) Mcallister, M. J.; Li, J.; Adamson, D. H.; Schniepp, H. C.; Abdala, A. a; Liu, J.; Herrera-alonso, O. M.; Milius, D. L.; Car, R.; Prud, R. K.; Aksay, I. a. Expansion of Graphite. *Society* **2007**, *19* (4), 4396–4404. https://doi.org/10.1021/cm0630800.

(41) Cao, Y.; Fatemi, V.; Fang, S.; Watanabe, K.; Taniguchi, T.; Kaxiras, E.; Jarillo-Herrero, P. Unconventional Superconductivity in Magic-Angle Graphene Superlattices. *Nat. 2018 5567699* **2018**, *556* (7699), 43–50. https://doi.org/10.1038/nature26160.

(42) Kim, H.; Abdala, A. A.; MacOsko, C. W. Graphene/Polymer Nanocomposites. *Macromolecules* **2010**, *43* (16), 6515–6530. https://doi.org/10.1021/MA100572E/ASSET/IMAGES/MEDIUM/MA-2010-00572E_0012.GIF.

(43) Steurer, P.; Wissert, R.; Thomann, R.; Mülhaupt, R. Functionalized Graphenes and Thermoplastic Nanocomposites Based upon Expanded Graphite Oxide. *Macromol. Rapid Commun.* **2009**, *30* (4–5), 316–327. https://doi.org/10.1002/MARC.200800754.

(44) Osman, M. A.; Mittal, V.; Morbidelli, M.; Suter, U. W. Polyurethane Adhesive Nanocomposites as Gas Permeation Barrier. *Macromolecules* **2003**, *36* (26), 9851–9858. https://doi.org/10.1021/MA035077X.

(45) Nelson, J. B.; Riley, D. P. The Thermal Expansion of Graphite from 15°c. to 800°c.: Part I. Experimental. *Proc. Phys. Soc.* **1945**, *57* (6), 477. https://doi.org/10.1088/0959-5309/57/6/303.

(46) Xu, Y.; Hong, W.; Bai, H.; Li, C.; Shi, G. Strong and Ductile Poly(Vinyl Alcohol)/Graphene Oxide Composite Films with a Layered Structure. *Carbon N. Y.* **2009**, *47* (15), 3538–3543. https://doi.org/10.1016/J.CARBON.2009.08.022.

(47) Salavagione, H. J.; Gómez, M. A.; Martínez, G. Polymeric Modification of Graphene through Esterification of Graphite Oxide and Poly(Vinyl Alcohol). *Macromolecules* **2009**, *42* (17), 6331–6334. https://doi.org/10.1021/MA900845W/SUPPL_FILE/MA900845W_SI_001.PDF.

(48) Keith, H. D.; Padden, F. J. Banding in Polyethylene and Other Spherulites. *Macromolecules* **1996**, *29* (24), 7776–7786. https://doi.org/10.1021/ma960634j.

(49) Keith, H. D.; Padden, F. J. Note on the Origin of Twisting Orientation in Fibrillar Crystals. *J. Polym. Sci.* **1961**, *51* (156), S4–S7. https://doi.org/10.1002/POL.1961.1205115616.

(50) *(PDF) Low density polyethylene-LDPE: Market, production, properties and applications*. https://www.researchgate.net/publication/316253852_Low_density_polyethylene-LDPE_Market_production_properties_and_applications/figures?lo=1 (accessed 2022-11-23).

(51) Keith, H. D.; Padden, F. J. The Optical Behavior of Spherulites in Crystalline Polymers. Part I. Calculation of Theoretical Extinction Patterns in Spherulites with Twisting Crystalline Orientation. *J. Polym. Sci.* **1959**, *39* (135), 101–122. https://doi.org/10.1002/pol.1959.1203913509.

(52) Twisted Crystals and the Origin of Banding in Spherulites of Semicrystalline Polymers. **2020**. https://doi.org/10.1021/acs.macromol.9b01567.

(53) Keith, H. D.; Padden, F. J. Twisting Orientation and the Role of Transient States in Polymer Crystallization. *Polymer (Guildf).* **1984**, *25* (1), 28–42. https://doi.org/10.1016/0032-3861(84)90264-7.

(54) Keith, H. D.; Padden, F. J.; Lotz, B.; Wittmann, J. C. Asymmetries of Habit in Polyethylene Crystals Grown from the Melt. *Macromolecules* **1989**, *22* (5), 2230–2238. https://doi.org/10.1021/MA00195A041/ASSET/MA00195A041.FP.PNG_V03.

(55) Chen, K.; Tang, X.; Jia, B.; Cho, C.; Wei, Y.; Chao, C.; Hou, J.; Dong, L.; Deng, X.; Xiao, T.-H.; Goda, K.; Guo, L. Graphene Oxide Bulk Material Reinforced by Heterophase Platelets with Multiscale Interface Crosslinking. https://doi.org/10.1038/s41563-022-01292-4.

(56) *MC 5 Micro compounders - Xplore Instruments*. https://www.xplore-together.com/products/micro-compounders-mc-5 (accessed 2022-11-25).

(57) Tao, Y.; Hinduja, S.; Heinemann, R.; Gomes, A.; Bártolo, P. J. A Study of Physico-Mechanical Properties of Hollow Glass Bubble, Jute Fibre and Rubber Powder Reinforced Polypropylene Compounds with and without MuCell ® Technology for Lightweight Applications. https://doi.org/10.3390/polym12112664.

(58) Di Gianfrancesco, A. Technologies for Chemical Analyses, Microstructural and Inspection Investigations. *Mater. Ultra-Supercritical Adv. Ultra-Supercritical Power Plants* **2017**, 197–245. https://doi.org/10.1016/B978-0-08-100552-1.00008-7.

(59) Corle, T. R.; Kino, G. S. Introduction. *Confocal Scanning Opt. Microsc. Relat. Imaging Syst.* **1996**, 1–66. https://doi.org/10.1016/B978-012408750-7/50009-4.

(60) *ZEISS Axioscope 5 Smart Laboratory Microscope*. https://www.zeiss.com/microscopy/en/products/light-microscopes/widefield-microscopes/axioscope-5.html (accessed 2022-12-01).

(61) Anilal, A.; Bendesky, J.; Jeong, S.; Lee, S. S.; Bozlar, M. Effects of Graphene on Twisting of High Density Polyethylene. *Proc. Am. Soc. Compos. Tech. Conf.* **2022**, *0* (0). https://doi.org/10.12783/ASC37/36468.

(62) Sherwood, P. M. A. Carbons and Graphites: Surface Properties Of. *Encycl. Mater. Sci. Technol.* **2001**, 985–995. https://doi.org/10.1016/B0-08-043152-6/00183-2.

(63) Raval, N.; Maheshwari, R.; Kalyane, D.; Youngren-Ortiz, S. R.; Chougule, M. B.; Tekade, R. K. Importance of Physicochemical Characterization of Nanoparticles in Pharmaceutical Product Development. *Basic Fundam. Drug Deliv.* **2019**, 369–400. https://doi.org/10.1016/B978-0-12-817909-3.00010-8.

(64) *Bragg's Law - Chemistry LibreTexts*. https://chem.libretexts.org/Bookshelves/Analytical_Chemistry/Supplemental_Modules_(Analytical_Chemistry)/Instrumentation_and_Analysis/Diffraction_Scattering_Techniques/Bragg's_Law (accessed 2022-12-08).

(65) *Bragg law | Definition, Equation, Diagram, & Facts | Britannica*. https://www.britannica.com/science/Bragg-law (accessed 2022-12-08).

(66) *X-ray Diffraction | XRD | XRPD | Malvern Panalytical*. https://www.malvernpanalytical.com/en/products/technology/xray-analysis/x-ray-diffraction (accessed 2022-12-08).

(67) *X'Pert^3 MRD XL | Research, Development & Quality Control XRD System | Malvern Panalytical*. https://www.malvernpanalytical.com/en/products/product-range/xpert3-range/xpert3-mrd-xl (accessed 2022-12-08).

(68) *Scanning Electron Microscopy - Nanoscience Instruments*. https://www.nanoscience.com/techniques/scanning-electron-microscopy/ (accessed 2022-12-03).

(69) *Scanning Electron Microscope - Radiological and Environmental Management - Purdue University*. https://www.purdue.edu/ehps/rem/laboratory/equipment safety/Research Equipment/sem.html (accessed 2022-12-03).

(70) *Scanning Electron Microscopes SU3800/SU3900*. https://www.hitachi-hightech.com/global/science/products/microscopes/electron-microscope/sem/su3800.html (accessed 2022-12-03).